Asian Journal of Chemistry; Vol. 34, No. 10 (2022), 2763-2770

ASIAN JOURNAL OF CHEMISTRY

https://doi.org/10.14233/ajchem.2022.24029

Anodization of Aluminium Alloys in Hydrofluoric Acid and Sulfuric Acid for Space Applications

SONIYA SOMASUNDARAM[1,2,3] and P. MURALI KRISHNA[2,3,*]

[1]Foundry & Forge Division, Hindustan Aeronautics Limited, Bangalore-560017, India
[2]Department of Chemistry, Ramaiah Institute of Technology, Bangalore-560054, India
[3]Visvesvaraya Technological University, Belagavi-590018, India

*Corresponding author: E-mail: muralikp@msrit.edu

Received: 18 August 2022; *Accepted*: 15 September 2022; *Published online*: 19 September 2022; AJC-20985

Present work demonstrated the development of a typical solar reflector coating by optimizing the bath parameters for an anodizing process on aluminium 2024 alloy. This evidently explains the pre-cleaning as well as optimization of the bath parameters for the development of solar reflector anodic film on aluminium alloys. The electrolytic bath for anodization consists of concentrated sulphuric acid and hydrofluoric acid. The anodization parameters such as solution temperature, process time and current density were optimized in order to achieve an anodic film of 10-12 μm thickness on the aluminium surface based on α/ε ratio, [solar absorbance (α) and thermal emittance (ε)] with a low solar absorbance (< 0.20) and high thermal emittance (> 0.80). The chemical analysis of the surface coating has been done by energy dispersive X-ray spectroscopy (EDS) and microstructure analysis by scanning electron microscopy (SEM). The finalized anodic film was compared with the sulphuric acid and chromic acid anodized surface. The average breakdown voltage of the solar reflector specimens coating was 355 V, which is higher than sulphuric acid anodized and chromic acid anodized samples.

Keywords: Aluminium 2024 alloy, Anodization, Thermooptical properties.

INTRODUCTION

Spacecrafts are designed to operate in all the extreme environmental conditions so that direct sun load is faced by one side of the spacecraft and deep cold space is faced by the other side. This creates the thermal gradient between the sun-light and shadowed sides of the spacecraft. The majority of the sub-systems of the vehicle operate at maximum efficiency within the specified temperature limit. Outside these limits, their life-time may be reduced. In the earthen atmosphere, temperature control can be achieved by heat exchange with the atmosphere. But in space, heat exchange is possible only through the radiation process. Hence, the temperature control of the subsystems can be achieved by adjusting the ratio of solar absorptance to infrared emittance of its surface. In order to achieve specified temperature limits, various coatings can be applied to the sub-systems. The absolute temperature of the spacecraft can be predicted using the following eqn. 1, which is related to the ratio of solar absorptance to infrared emittance [1].

$$T_{s/c} = \sqrt[4]{\frac{S\alpha A_p}{\sigma \varepsilon A}} \quad (1)$$

where, $T_{s/c}$ is the absolute temperature of the spacecraft, S is the solar constant (mean value 1353 W/m^2), σ is the Stefan Boltzmann constant (56.7×10^{-9} W/m^{-2} K^{-1}), A_p is the projected surface area of the spacecraft perpendicular to the solar rays (m^2), A is the total surface area of the spacecraft (m^2), α is the solar absorptance and ε is the infrared emittance of the surface. Since S, σ, A_p and A are constant, it can be derived that the temperature of the spacecraft is proportional to the α/ε ratio. Different surface protective coatings were employed to control the temperature as well as corrosion of the spacecraft parts by controlling the α/ε ratio. Since, the spacecraft is not approachable to repair in its orbit, it is always better to provide the surface finish to control the temperature limits. Based on their optical properties, thermal control coatings can be divided into four major groups. They are solar reflectors (low α, high ε), solar absorbers (high α, low ε), flat reflectors (low α, low ε) and flat absorbers (high α, high ε).

In space technology, solar reflector coatings were developed on high-strength aerospace aluminium alloys, such as AA2024T3 in the form of an anodic oxide layer by electrolytic anodization method [2-5]. Anodization of aluminium alloy

can be done with a large range of electrolytes using AC or DC current or a combination of both. On anodization, improves the tough, corrosion as well as abrasion-resistant oxide coating on aluminium alloys [6,7]. In addition, anodizing provides the required optical properties (high emissivity and low absorptivity) to minimize thermal cycling temperature and prevent overheating and undercooling in every part of the spacecraft [8-10].

The anodic oxidation method in a mixed acid system was adopted in present work and the anodized AA2024 alloy was obtained with a lower α/ε ratio. The study of different bath parameters like electrolytic concentration, temperature, time, current density, *etc*. was done and finally developed the anodic oxidation process of Al 2024 alloys to get a solar reflector surface. These are reflectors, that reflect the incident solar energy back into space. Thermal control of the satellite is mainly achieved by isolating it from the harsh environment of space. This can be achieved by employing different types of coatings. In the development of coatings, not only the current density but also the electrolytic composition and sample surface were also important factors, which deeply influence the coating technology. The addition of two or more different acids as an electrolyte served as a renewed electrolyte. Studies have proved that the addition of some organic or inorganic compounds is an effective method to regulate the anodization process and hence the coating morphology [11-13].

Literature shows that during the anodization process, the most commonly used electrolytes reported are inorganic acids such as chromic acid (type 1 used for corrosion resistance and good paint adhesion) [14,15] or sulphuric acid (type 2 for colouring) [16-22], phosphoric/pyrophosphoric acid [23-25], selenic acid [26,27], boric acid [28] and organic acids such as malonic acid [29-31], oxalic acid [32-34], citric acid [28,35, 36], malic acid [37], tartaric acid [38,39], formic acid [40], glycolic acid [41], glutaric acid and its derivatives [42] and also a mixture of acids such as phosphoric acid and oxalic acid [43], sulphuric acid and boric acid [44-48] (or) tartaric acid [49-53] (or) citric acid [54], malonic acid [55]. However, best of our knowledge, there is no literature available on using a mixture of sulphuric acid and hydrofluoric acid.

In the light of the above, as a continuation of our study on thermal coatings [56], herein reporting the development of solar reflector anodic film with low α and high ε values on aluminium alloys in an electrolytic mixture containing H_2SO_4 and HF, then investigated the effect of parameters like solution temperature, process time, current density and electrolyte concentrations.

EXPERIMENTAL

All the solutions used were prepared by adding appropriate amounts of laboratory-grade chemicals using de-mineralized water. The chemicals *viz*. trichloroethylene, sodium carbonate, trisodium orthophosphate, sodium lauryl sulphate, sodium hydroxide, sulphuric acid (98%), hydrofluoric acid (40%), nitric acid (69%) and orthophosphoric acid (85%) were procured from the reliable commercial sources.

The microstructure of the coatings was determined by scanning electron microscopy (Carl Zeiss, EVO 18 Research) and the energy dispersive X-ray spectroscopy (EDS) (Oxford) was employed to study and compare the surface morphology and elemental analysis of the anodized samples. The Thermo optical properties such as solar absorptance (α_s) and infrared emittance (ε_R) of the anodic coating were measured using an emissometer (Devices and services Co., USA) and solar spectrum reflectometer (Devices and services Co., USA). Coating thickness measurements were done using the dual scope meter (Helmut Fisher thickness meter). The universal hardness tester (Indentec) was used to measure the hardness of the coatings. The breakdown voltage of the specimens was tested using a Zeal breakdown voltage tester.

Composition, cleaning and preparation of the alloy sample: A deliberated specimen of aluminium alloy (AA2024) whose chemical composition was analyzed using an optical emission spectrometer (Thermofisher Model: ARL 3460) as shown in Table-1. The aluminium alloy samples (40 mm × 40 mm × 5 mm) were pre-cleaned before anodization using the following steps: The aluminium specimens were degreased or cleaned using trichloroethylene in an ultrasonic bath for 10 min at room temperature (25 ± 5 ºC). The alloys were etched for 60 s in an alkaline solution containing sodium carbonate (150 g/L), trisodium orthophosphate (120 g/L) and sodium lauryl sulphate (1 g/L) and sodium hydroxide (60 g/L) at 60 ± 5 ºC. After alkaline cleaning, the substrates were thoroughly washed with de-mineralized water and dried.

The substrate was then desmutted for 60 s by dipping in a solution containing sulphuric acid (98%, 650 mL/L), hydrofluoric acid (40%, 1 mL/L) and nitric acid (70%, 250 mL/L) at room temperature (25 ± 5 ºC) and followed by cleaning with de-mineralized water. Finally, the substrates were cleaned with chemical solution containing orthophosphoric acid (85%, 800 mL/L), nitric acid (70%, 35 mL/L) and copper (99.9%, 0.1 g/L) at 90 ± 2 ºC for 30 s followed by thorough rinsing with de-mineralized water.

Anodizing and sealing: A mixed acid electrolyte with a different combination of sulphuric acid and hydrofluoric acid was used as the anodizing electrolyte. Anodizing is done with a square wave pulsed direct current rectifier. The optimization studies of the process were done by varying the thickness, current density, time, temperature and concentration of electrolytes. The maintenance of bath temperature was performed by using a chiller unit (Julabo Model: F34). Pure lead (99.9%) was used as a cathode in the anodizing process. Sealing was done in hot distilled water (> 98 ºC) for 1 h. The pH of the water was maintained at 6.5-7.0. The sulphuric acid and chromic

TABLE-1
COMPOSITION OF ALUMINIUM 2024 ALLOY IN WEIGHT (%)

Component	Cu	Fe	Mg	Mn	Si	Cr	Ti	Zn	Al
Weight (%)	4.50	0.12	1.43	0.49	0.05	0.01	0.02	0.02	93.31

acid anodized samples used for the comparison with finalized solar reflector coatings were prepared as per bath parameters given in Table-2.

TABLE-2
BATH COMPOSITION AND PARAMETERS FOR SULPHURIC ACID AND CHROMIC ACID ANODIZATION

Parameters	Sulphuric acid (210 g/L)	Chromic acid (40 g/L)
Temperature (°C)	25 ± 5	40 ± 5
Average current density (A/dm^2)	20	0.6
Time for plating (min)	20	50

Optical properties: The thermooptical properties such as solar absorptance (α_s) and infrared emittance (ε_R) of the anodic coating were measured using an emissometer and solar spectrum reflectometer, respectively. In a solar spectrum reflectometer, a tungsten lamp was used as a source of illumination. A reflected radiation from the surface of the sample is measured at an angle of 20º from the normal with four detectors. Summing up these outputs gives the solar absorptance of the sample. The emissometer was used to measure the emittance of a surface wherein the maximum working temperature of the collector is in the range of 80-85 ºC. The detector of the emissometer consists of a thermopile with low and high emittance areas, which ensures the measurement of the emissivity of the surface. The ratio of α/ε is calculated after each trial to study the effect of different parameters on the optical property of the coating.

Morphological and microhardness studies: The SEM images were recorded at a voltage of 20 KV and a secondary electron detector was used. A comparison of the chemical composition and microhardness of solar reflector coating was done with sulphuric acid, chromic acid anodized and bare aluminium 2024 alloy samples using a Universal hardness tester.

Breakdown voltage test: For some power-driven applications of aluminium, where the requirements of conductivity are involved, the breakdown voltage is a very important parameter to be measured. Hence, it is measured for the finalized solar reflector coating and compared with other available coatings. The breakdown voltage of the reflector coating was measured using a ZEAL Breakdown voltage tester.

RESULTS AND DISCUSSION

Anodizing is an electrochemical process used to coat oxide film on metal surfaces. Anodization layer on AA2024 alloys developed, which acts as a solar reflector coating and is used widely in spacecraft thermal control applications. In present work, anodization was carried out in sulphuric and hydrofluoric acid mixture and evaluated for the optimization of the current density, duration of the treatment, bath temperature, concentration of acids *etc*. to meet the optical properties of the coating.

Anodization process optimization: The optimization of the anodization process was carried out by varying the electrolyte mixture of sulphuric acid and hydrofluoric acid. The process was carried out to investigate the influence of coating thickness and various operating parameters *viz*., current density, time of the process, bath temperature and electrolyte concentration on thermo optical properties of the coating. The development of a coating over aluminium 2024 alloy of 10-12 μm thickness to assure the sustainability of the coating. The desired coating was characterized by the scanning electron microscope equipped with energy dispersive X-ray spectroscopy and microhardness and results were compared with the chromic acid and sulphuric acid anodized coating as well as bare (non-anodized) samples.

Effect of anodic coating thickness on solar reflector coating: Emittance is the surface phenomenon which indicates the emittance in the infrared region, when an anodized layer is formed on the specimen, the IR emittance increases with the increase in thickness and solar absorbance decreases. The solar reflector property depends upon the α/ε ratio of the surface. Hence the thickness is varied to optimize the α/ε ratio as the minimum to maintain the solar reflector properties. Fig. 1a shows the variation of solar absorbance and IR emittance with respect to the coating thickness. There is a slow increase in the α value of the coating and at the same time, there is a sharp rise in the IR emittance with an increase in thickness. The ratio of α/ε obtained for the thickness of 5 μm and 10 μm is comparable. Hence, the optimum thickness for the solar reflector coating is finalized at 10 ± 2 μm, which gives a stable anodized layer compared to the anodic layer of thickness of 5 μm.

Effect of current density: To understand the effect of current density on the optical properties of the coating, trials were conducted at various constant current densities varying from 2 A/ft^2 to 10 A/ft^2. The electrolyte concentration was maintained as 175 g/L sulphuric acid and 1 mL/L hydrofluoric acid at room temperature (25 ± 5 ºC). At lower current density, the rate of anodic film formation was low and the coating obtained was having poor absorbance and emittance. But at a higher current density, the appearance of the coating resembles the normal sulphuric acid anodized samples and the α/ε ratio was increased to an extent which never meets the requirements of solar reflector coating. Fig. 1b shows the effect of current density on the α and ε values of the coating. The lowest α/ε ratio was obtained at a current density of 40 A/ft^2.

Effect of process time: The effect of the anodization process time was monitored by carrying out in different time intervals between 5 to 60 min (Fig. 1c). As the processing time increases thickness and α/ε ratio also increases. However, the minimum α/ε value was obtained in 5 min, as the appreciable coating thickness is not obtained in 5 min the processing time was fixed to 10 min.

Effect of electrolytic temperature: The electrolyte bath temperature controls the appearance as well as optical properties of the anodic coating. Hence, the temperature plays an important role in the anodization process. To monitor the effect of temperature on the bath, the anodization process was carried out from 0 to 25 ºC. The temperature of the bath was maintained by using a chiller unit. The results of the temperature effect are shown in Fig. 1d and the combination of sulphuric acid and hydrofluoric acid temperature does not show any effect on the formation of coating thickness and hence optical properties.

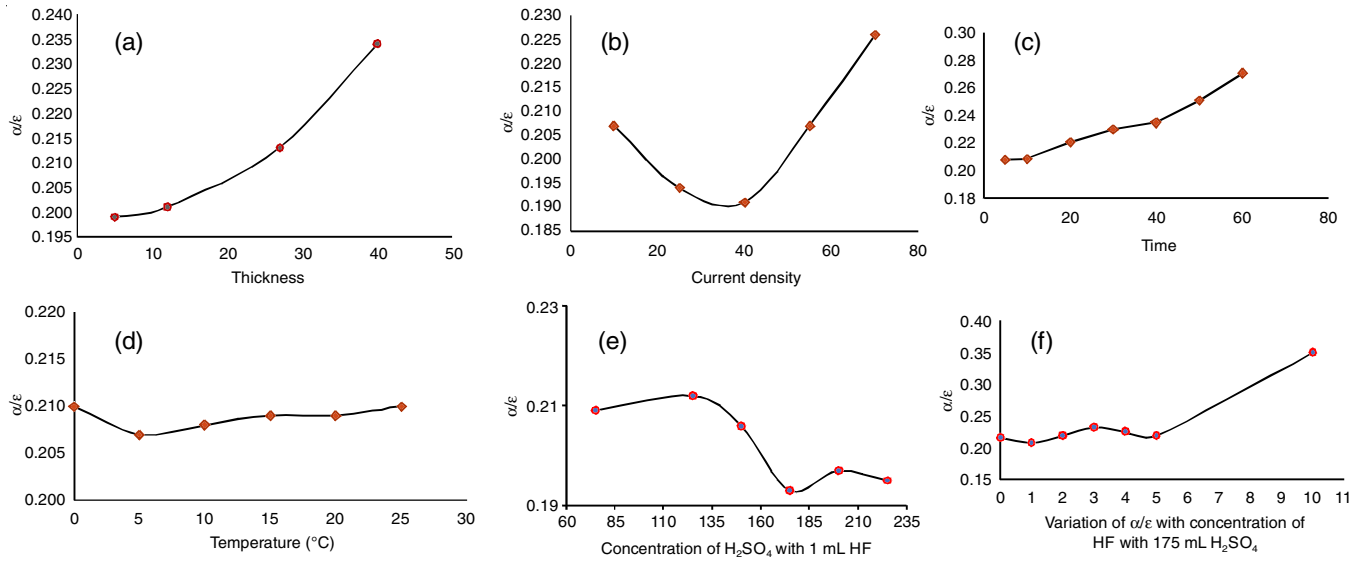

Fig. 1. Variation of α/ε values with change in (a) thickness, (b) current density, (c) time, (d) temperature, (e) concentration of H_2SO_4 in 1 mL HF, (f) concentration of HF in 175 mL H_2SO_4

Effect of concentration of sulphuric acid and hydrofluoric acid: The effect of the concentrations of electrolytic bath mixture on the anodization process was investigated by taking the different volumes of the sulphuric acid (75 to 275 mL/L) and hydrofluoric acid (0 to 5 mL/L) to optimize for the desired optical properties. The addition of hydrofluoric acid causes the activation of the alloy surface by thinning the existing oxide film and enables the oxidation of aluminium alloy thereby formation of the coating to proceed. The addition of fluoride ions to the electrolyte also causes for achieving a large reduction in the anodizing voltage [13]. In order to fix the volume of sulphuric acid, the volume of hydrofluoric acid was fixed to 1 mL/L and varied the volume of the sulphuric acid was from 75 to 275 mL/L. From Fig. 1e, data indicate that an increase in the concentration of sulphuric acid from 75 mL to 175 mL/L shows the decrease in α/ε values and then remains constant further. Similarly, to fix the concentration of hydrofluoric acid, the concentration of sulphuric acid is kept at 175 mL/L and varied the concentration of hydrofluoric acid is from 0 to 10 mL/L. Fig. 1f shows that the addition of 1 mL of hydrofluoric acid to 175 mL/L sulphuric acid bath shows the lowest α/ε value. Further addition of hydrofluoric acid has increased the α/ε values. In these studies, the current density applied was 40 A/ft^2 for 10 min at room temperature (20 ± 5 ºC). Based on the data obtained for various parameters, the optimum parameters of the electrolytic bath are shown in Table-3.

TABLE-3
FINALIZED PARAMETERS FOR ANODIZING

Electrolytic composition	
Sulphuric acid	175 mL/L
Hydrofluoric acid	1 mL/L
Process parameters	
Temperature	25 ± 5 °C
Average current density	40 A/ft^2
Time for anodizing	10 min

Evaluation of the coating

Visual inspection: All the anodized specimens were visually examined with the unaided eye as well as under a magnification of 15× using a stereo microscope. The coatings were found to be continuous, smooth and uniformly white in colour with no loose films, breaks, scratches, cracks, patches or other defects.

Thickness measurement: The anodized samples over aluminium 2024 substrates were sectioned using diamond cutting wheel. The sectioned surface was then metallographic polished with 220 grit, 340 grit and 600 grit emery sheets. The samples were then polished with alumina (particle size 0.3 µm and 0.05 µm) suspended solutions to have a smooth uniform surface and then subjected to SEM analysis to measure the plating thickness. The anodizing thickness was found to be around 10 to 12 µm. The thickness of the anodic coating was confirmed by the eddy current method using a thickness tester. This instrument employs a probe coil carrying an RF alternating current.

Composition of the coating: The EDS analysis of the anodic surface obtained at different concentrations of sulphuric acid and hydrofluoric acid were compared with each other as well as with normal sulphuric acid anodized and chromic acid anodized samples. Table-4 shows the elemental composition (EDS) of anodic coatings at different concentrations of sulphuric acid and without the addition of hydrofluoric acid to the bath. With an increase in the concentration of sulphuric acid, there is a gradual increase in the concentration of elemental oxygen as well as sulphur with a reduction in the aluminium percentage.

This clearly shows the increase in the rate of anodizing with an increase in the concentration of sulphuric acid. But with the addition of hydrofluoric acid to the bath, there is no prominent change in the concentration of elemental oxygen and sulphur. At the same time, there is a gradual increase in the elemental concentration of fluoride in the coating. From the different parametric studies, the concentration of sulphuric acid is fixed at 175 mL/L and the studies continued to under-

TABLE-4
ELEMENTAL COMPOSITION (EDS) OF ANODIC COATINGS AT DIFFERENT CONCENTRATIONS OF H_2SO_4 AND WITH/WITHOUT HF

Conc. of H_2SO_4 in bath (mL/L)	Conc. of HF in bath (mL/L)	Elemental composition (%)			
		O	Al	S	F
75	0	48.7	46.0	5.2	–
125	0	49.0	45.0	6.0	–
175	0	49.3	43.9	6.8	–
225	0	49.5	43.1	7.4	–
275	0	49.6	42.4	7.9	–
325	0	49.8	42.0	8.0	–
175	1	46.3	46.8	6.4	0.1
175	2	48.9	44.3	6.0	0.7
175	3	53.3	39.8	5.8	1.0
175	4	54.8	39.3	4.8	1.2
175	5	52.9	41.3	4.6	1.2
175	10	11.5	88.2	0.1	0.2

stand the effect of hydrofluoric acid inclusion in the bath. Table-4 shows the elemental composition (EDS) of anodic coatings at a fixed concentration of sulphuric acid and different concentrations of hydrofluoric acid. The addition of a small amount of hydrofluoric acid to the bath has shown a drastic change of α/ε value of the coating. But increase in the addition of hydrofluoric acid does not have any effect on the α/ε values of the coating. So, the addition of minimal hydrofluoric acid is preferred for the achievement of solar reflector coating.

SEM studies: Fig. 2 shows the comparison of scanning electron images of solar reflector coatings with a gradual increase in the concentration of hydrofluoric acid. Fig. 3 shows the comparison of SEM images of the optimized solar reflector coating with sulphuric acid and chromic acid anodized aluminium alloy samples along with bare AA2024 alloy. There is a clear difference in the pattern of an anodized layer of solar reflector coating when compared to sulphuric acid and chromic acid anodized coatings. The flakier structure of solar reflector coating led to the differential optical properties of the optimized coating. This flaky structure increases with the addition of hydrofluoric acid up to 3 mL, but further addition of hydrofluoric acid leads to a structure similar to the normal sulphuric acid anodized sample. The increase in flaky structure has also led to the increase in absorptance value and results in a high α/ε ratio.

Microhardness studies: Since the thickness of the coating was very less, the hardness value obtained was found to be almost the same as the bare sample. Hence, the microhardness values were compared to bare aluminium 2024, sulphuric acid anodized and chromic acid anodized samples. The reason for the lowest microhardness value of the solar reflector may be due to the low thickness of the developed coating. The microhardness value of the chromic acid anodized layer is found to be better than the bare sample (Table-5). Similarly, the microhardness values of the sulphuric acid anodized samples were better than the chromic acid anodized.

Microhardness measurements of the samples were done on the surface and this may cause interference with the base material. The microhardness of the anodized layer is a bit difficult to measure since the thickness of the layer is very small and the impact of the base metal is inevitable. So, the above-said values may not be proper with respect to the anodic layer.

Breakdown voltage studies: The breakdown voltage of the reflector coating was measured and compared with the sulphuric acid and chromic acid anodized samples. High voltage is applied across the insulated specimens and find out the

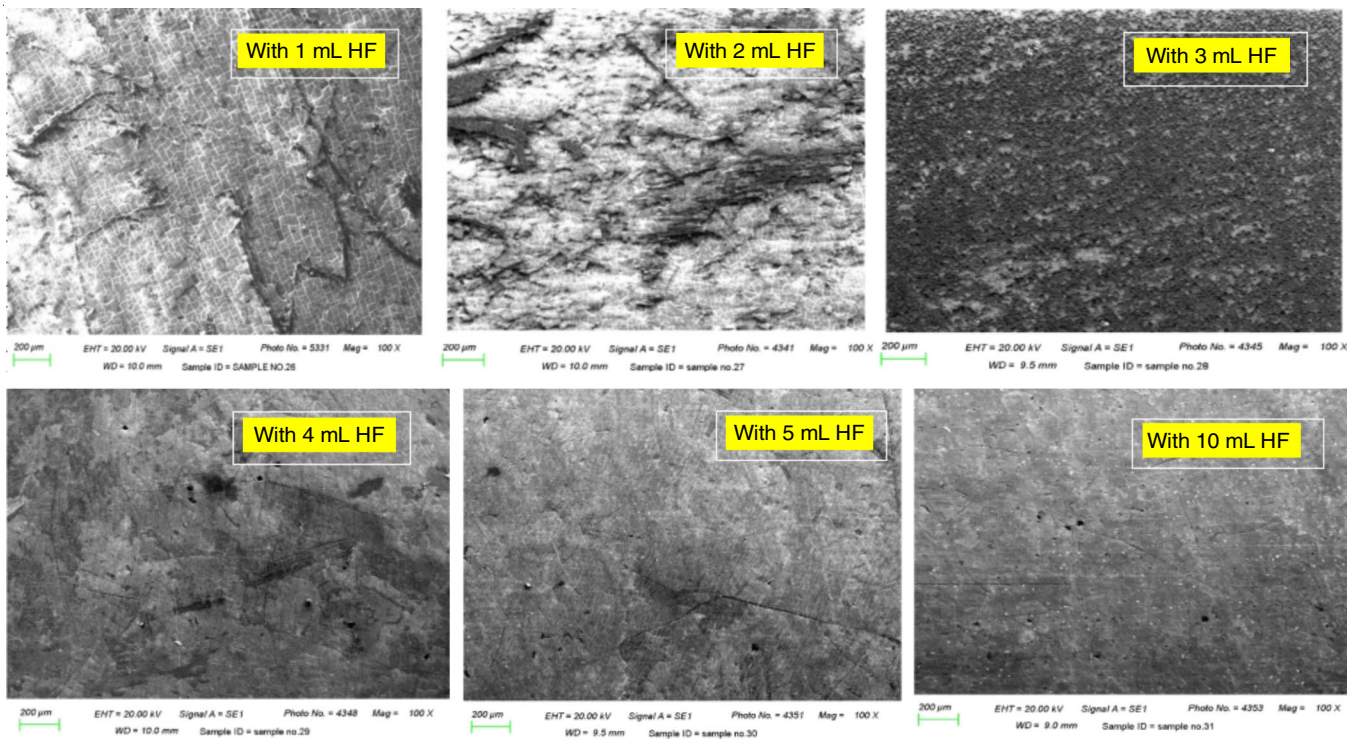

Fig. 2. Scanning electron microscope images of solar reflector coatings with a gradual increase in the concentration of hydrofluoric acid

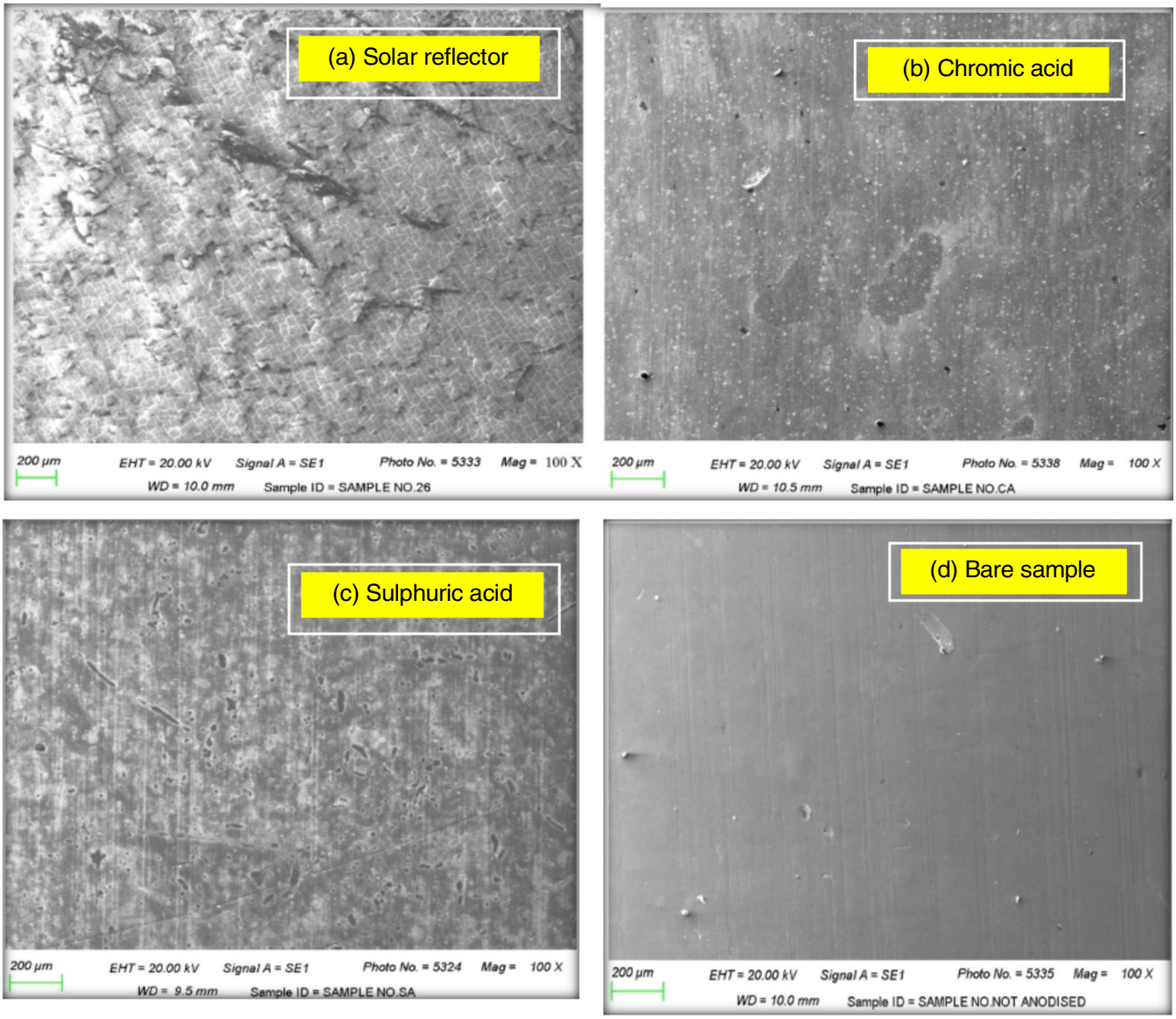

Fig. 3. Scanning electron microscope images of the (a) finalized solar reflector coating, (b) chromic acid anodized coating, (c) sulphuric acid anodized coating and (d) bare aluminium 2024 alloy samples

TABLE-5
COMPARISON OF VICKERS HARDNESS VALUES

Material type	Microhardness (VHN)	Average
Bare Al 2024 sample	77.2 79.4 80.4	79
Chromic acid anodized sample	86.8 89.1 89.3	88
Sulphuric acid anodized sample	122.7 121.3 121.1	122
Solar reflector sample	75.8 82.3 81.5	80

breakdown voltage of the specimen, further which voltage will not increase in the tester. It is understood that the breakdown voltage of sulphuric acid anodized samples will be around 200 to 300 V and for the chromic acid anodized samples the breakdown will happen at the voltage of 50 V (Table-6). Hard anodizing is the hardest coating process, which gives a breakdown voltage of 800 to 1000 V. The solar reflector coatings

TABLE-6
BREAKDOWN VOLTAGE READINGS
FOR SOLAR REFLECTOR COATING

S. No.	Breakdown voltage (V)	S. No.	Breakdown voltage (V)
1	360	9	430
2	350	10	430
3	330	11	460
4	250	12	420
5	270	13	360
6	330	14	440
7	350	15	280
8	410	16	310
Average: 335			

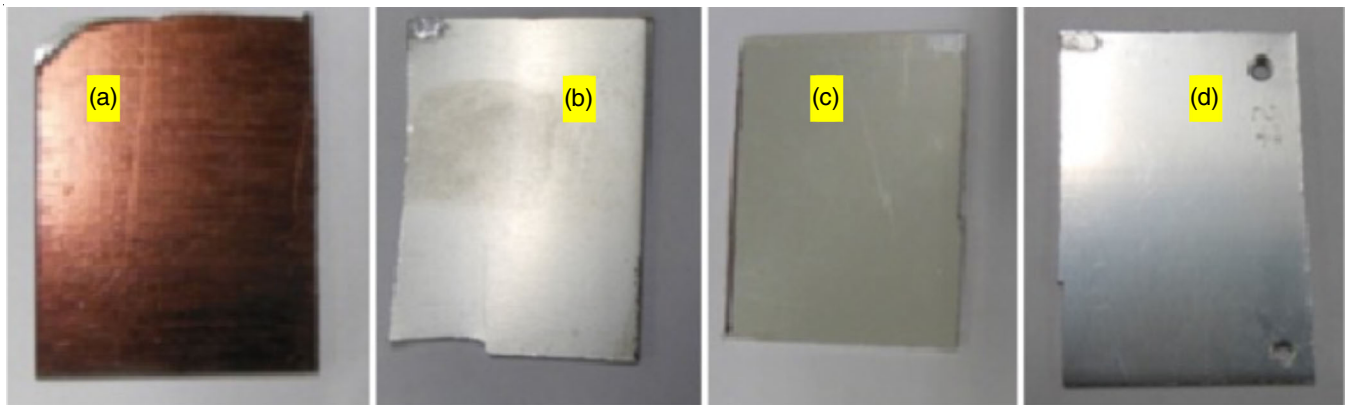

Fig. 4. Comparison of the different types of anodic coatings with a solar reflector coating (a) hard anodized, (b) sulphuric acid, (c) chromic acid, (d) solar reflector coating

were checked for its breakdown voltage. It has a breakdown voltage from 250 to 440 V. The average breakdown voltage of the said coating is 355 V, which is higher than sulphuric acid anodized and chromic acid anodized samples.

Optical properties: During the thickness variation studies, the lowest α/ε value was obtained at a thickness of 10 µm anodized layer. Similarly, the lowest α/ε values were obtained at 40 A/ft^2 current density, 10 min process time, 20 ± 5 ºC temperature and 175 mL/L sulphuric acid and 1 mL/L hydrofluoric acid electrolyte. Each parameter was finalized based on the evaluation of the optical properties of the coating. The optical properties of the solar reflector coating were compared with the various anodized coatings such as white paint, black paint, aluminium paint, hard anodizing, chromic acid and sulphuric acid anodizing coating (Table -7) and the data indicate the developed solar reflector coating is superior to the other existing anodized coatings. The appearance of the existing anodic coatings is compared with a developed solar reflector coating (Fig. 4).

TABLE-7
COMPARISON OF OPTICAL PROPERTIES OF SOLAR REFLECTOR COATING WITH OTHER AVAILABLE COATINGS

Type of coating	α	ε	α/ε
White paint	0.20	0.90	0.222
Black paint	0.95	0.90	1.05
Aluminium paint	0.25	0.25	1.00
Hard anodizing	0.90	0.90	1.00
Chromic acid anodizing	0.60	0.30	2.00
Normal sulphuric acid anodizing	0.32	0.78	0.41
Solae reflector coating	0.16	0.83	0.193

Conclusion

In summary, a solar reflector anodic coating on aluminium 2024 alloy was obtained in an electrolytic system containing 175 mL/L sulphuric acid and 1 mL hydrofluoric acid. The operating temperature was 20 ± 5 °C at a current density of 40 A/ft^2 for 10 min. This process provides the solar reflector coating with the lowest α/ε value, suitable for thermal control applications. A drop in the solar absorptance value of anodic coating is obtained by the addition of 1 mL/L hydrofluoric acid in the sulphuric acid anodizing solution. The optimized process provides highly reproducible results. A solar reflector coating with a thickness of 10-12 µm is obtained under optimized parameter conditions. Flaky structure or morphology of the developed solar reflector coating is compared with the smooth structure of the sulphuric acid and chromic acid anodized samples. This uneven, flaky structural pattern is the apparent reason for the achievement of lowest α/ε value (solar reflector) coating. Microhardness of the developed solar reflector coating is found to be 80 VHN and compared with the bare sample, hard anodized, sulphuric acid and chromic acid anodized samples. The breakdown voltage of the solar reflector coating was found in the range of 250-460 V and better when compared to the chromic acid and sulphuric acid anodizing.

ACKNOWLEDGEMENTS

The authors thank A. Rajendra and Anju M. Pillai, Thermal Systems Group, ISRO Satellite Centre, Bangalore, India for supporting in carrying this work. The authors also thank Indian Space Research Organization (ISRO) for financial support. The authors also thank the Centre for Advanced Material Technology and Department of Chemistry, Ramaiah Institute of Technology, Bangalore, India for some laboratory facilities.

CONFLICT OF INTEREST

The authors declare that there is no conflict of interests regarding the publication of this article.

REFERENCES

1. J. Meseguer, I. Pérez-Grande and A. Sanz-Andrés, Spacecraft Thermal Control, Elsevier: New York (2012).
2. C. Siva Kumar, S.M. Mayanna, K.N. Mahendra, A.K. Sharma and R. Uma Rani, *Appl. Surf. Sci.*, **151**, 280 (1999); https://doi.org/10.1016/S0169-4332(99)00290-1
3. C. Siva Kumar, A.K. Sharma, K.N. Mahendra and S.M. Mayanna, *Sol. Energy Mater. Sol. Cells*, **60**, 51 (2000); https://doi.org/10.1016/S0927-0248(99)00062-8
4. F. Li, L. Zhang and R.M. Metzger, *Chem. Mater.*, **10**, 2470 (1998); https://doi.org/10.1021/cm980163a
5. M.P. Martínez-Viademonte, S.T. Abrahami, T. Hack, M. Burchardt and H. Terryn, *Coatings*, **10**, 1106 (2020); https://doi.org/10.3390/coatings10111106
6. Y. Shang, L. Wang, Z. Liu, D. Niu, Y. Wang and C. Liu, *Int. J. Electrochem. Sci.*, **11**, 5234 (2016); https://doi.org/10.20964/2016.06.85

7. H.A. Elkilany, M.A. Shoeib and O.E. Abdel-Salam, *Metallogr. Microstruct. Anal.*, **8**, 861 (2019); https://doi.org/10.1007/s13632-019-00594-5
8. J. Park, K. Son, J. Lee, D. Kim and W. Chung, *Symmetry*, **13**, 433 (2021); https://doi.org/10.3390/sym13030433
9. A.M.A. El-Hameed, Y.A. Abdel-Aziz and F.S. El-Tokhy, *Mater. Sci. Appl.*, **8**, 197 (2017); https://doi.org/10.4236/msa.2017.82013
10. H. Dursch, Chromic acid Anodizing of Aluminium Foil, NASA Contract NAS1-1822 (1988).
11. R. Giovanardi, C. Fontanesi and W. Dallabarba, *Electrochim. Acta*, **56**, 3128 (2011); https://doi.org/10.1016/j.electacta.2011.01.065
12. W. Chen, J.S. Wu and X.H. Xia, *ACS Nano*, **2**, 959 (2008); https://doi.org/10.1021/nn700389j
13. R. Elaish, M. Curioni, K. Gowers, A. Kasuga, H. Habazaki, T. Hashimoto and P. Skeldon, *Electrochim. Acta*, **245**, 854 (2017); https://doi.org/10.1016/j.electacta.2017.06.034
14. S.J. Garcia-Vergara, P. Skeldon, G.E. Thompson and H. Habazaki, *Surf. Interface Anal.*, **39**, 860 (2007); https://doi.org/10.1002/sia.2601
15. W.J. Stêpniowski, M. Michalska-Domañska, M. Norek and T. Czujko, *Mater. Lett.*, **117**, 69 (2014); https://doi.org/10.1016/j.matlet.2013.11.099
16. H. Asoh, K. Nishio, M. Nakao, A. Yokoo, T. Tamamura and H. Masuda, *J. Vac. Sci. Technol. B*, **19**, 569 (2001); https://doi.org/10.1116/1.1347039
17. G.D. Sulka, S. Stroobants, V. Moshchalkov, G. Borghs and J.-P. Celis, *J. Electrochem. Soc.*, **149**, D97 (2002); https://doi.org/10.1149/1.1481527
18. G.D. Sulka and K.G. Parkola, *Thin Solid Films*, **515**, 338 (2006); https://doi.org/10.1016/j.tsf.2005.12.094
19. H. Masuda, F. Hasegwa and S. Ono, *J. Electrochem. Soc.*, **144**, L127 (1997); https://doi.org/10.1149/1.1837634
20. G.D. Sulka and K.G. Parkola, *Electrochim. Acta*, **52**, 1880 (2007); https://doi.org/10.1016/j.electacta.2006.07.053
21. S. Feliu Jr., M.J. Bartolomé, J.A. González, V. López and S. Feliu, *Appl. Surf. Sci.*, **254**, 2755 (2008); https://doi.org/10.1016/j.apsusc.2007.10.015
22. M. Curioni, M. Saenz de Miera, P. Skeldon, G.E. Thompson and J. Ferguson, *J. Electrochem. Soc.*, **155**, C387 (2008); https://doi.org/10.1149/1.2931522
23. A.P. Li, F. Müller and U. Gösele, *Electrochem. Solid-State Lett.*, **3**, 131 (2000); https://doi.org/10.1149/1.1390979
24. K. Surawathanawises and X. Cheng, *Electrochim. Acta*, **117**, 498 (2014); https://doi.org/10.1016/j.electacta.2013.11.144
25. D. Nakajima, T. Kikuchi, T. Yoshioka, H. Matsushima, M. Ueda, R.O. Suzuki and S. Natsui, *Materials*, **12**, 3497 (2019); https://doi.org/10.3390/ma12213497
26. T. Kikuchi, O. Nishinaga, S. Natsui and R.O. Suzuki, *Electrochim. Acta*, **137**, 728 (2014); https://doi.org/10.1016/j.electacta.2014.06.078
27. O. Nishinaga, T. Kikuchi, S. Natsui and R.O. Suzuki, *Sci. Rep.*, **3**, 2748 (2013); https://doi.org/10.1038/srep02748
28. S. Stojadinovic, R. Vasilic, Z. Nedic, B. Kasalica, I. Belca and L. Zekovic, *Thin Solid Films*, **519**, 3516 (2011); https://doi.org/10.1016/j.tsf.2011.01.188
29. W. Lee, K. Nielsch and U. Gösele, *Nanotechnology*, **18**, 475713 (2007); https://doi.org/10.1088/0957-4484/18/47/475713
30. J. Ren and Y. Zuo, *Appl. Surf. Sci.*, **261**, 193 (2012); https://doi.org/10.1016/j.apsusc.2012.07.139
31. I. Vrublevsky, A. Jagminas, S. Hemeltjen and W. Goedel, *J. Solid State Electrochem.*, **13**, 1873 (2009); https://doi.org/10.1007/s10008-008-0765-2
32. L. Zaraska, W.J. Stêpniowski, M. Jaskula and G.D. Sulka, *Appl. Surf. Sci.*, **305**, 650 (2014); https://doi.org/10.1016/j.apsusc.2014.03.154
33. G.D. Sulka and W.J. Stepniowski, *Electrochim. Acta*, **54**, 3683 (2009); https://doi.org/10.1016/j.electacta.2009.01.046
34. R. Zhang, K. Jiang, Y. Zhu, H. Qi and G. Ding, *Appl. Surf. Sci.*, **258**, 586 (2011); https://doi.org/10.1016/j.apsusc.2011.08.041
35. Y. Katsuta, A. Yasumori, K. Wada, K. Kurashima, S. Suehara and S. Inoue, *J. Non-Cryst. Solids*, **354**, 451 (2008); https://doi.org/10.1016/j.jnoncrysol.2007.06.085
36. S. Ono, M. Saito and H. Asoh, *Electrochim. Acta*, **51**, 827 (2005); https://doi.org/10.1016/j.electacta.2005.05.058
37. T. Kikuchi, T. Yamamoto and R.O. Suzuki, *Appl. Surf. Sci.*, **284**, 907 (2013); https://doi.org/10.1016/j.apsusc.2013.08.044
38. V.F. Surganov and G.G. Gorokh, *Mater. Lett.*, **17**, 121 (1993); https://doi.org/10.1016/0167-577X(93)90069-A
39. I.A. Vrublevsky, K.V. Chernyakova, A. Ispas, A. Bund and S. Zavadski, *Thin Solid Films*, **556**, 230 (2014); https://doi.org/10.1016/j.tsf.2014.01.074
40. T. Fukushima, Y. Fukuda, G. Ito and Y. Sato, *J. Surface Finishing Soc. Japan*, **21**, 319 (1970).
41. S.Z. Chu, K. Wada, S. Inoue, M. Isogai, Y. Katsuta and A. Yasumori, *J. Electrochem. Soc.*, **153**, B384 (2006); https://doi.org/10.1149/1.2218822
42. D. Nakajima, T. Kikuchi, S. Natsui and R.O. Suzuki, *Appl. Surf. Sci.*, **321**, 364 (2014); https://doi.org/10.1016/j.apsusc.2014.10.014
43. T.T. Kao and Y.C. Chang, *Appl. Surf. Sci.*, **288**, 654 (2014); https://doi.org/10.1016/j.apsusc.2013.10.091
44. L. Domingues, J.C.S. Fernandes, M. Da Cunha Belo, M.G.S. Ferreira and L. Guerra-Rosa, *Corros. Sci.*, **45**, 149 (2003); https://doi.org/10.1016/S0010-938X(02)00082-3
45. G.E. Thompson, L. Zhang, C.J.E. Smith and P. Skeldon, *Corrosion*, **55**, 1052 (1999); https://doi.org/10.5006/1.3283942
46. L. Zhang, G.E. Thompson, M. Curioni and P. Skeldon, *J. Electrochem. Soc.*, **160**, C179 (2013); https://doi.org/10.1149/2.032306jes
47. J. Zhang, X. Zhao, Y. Zuo and J. Xiong, *Surf. Coat. Technol.*, **202**, 3149 (2008); https://doi.org/10.1016/j.surfcoat.2007.10.041
48. M. Saeedikhani, M. Javidi and A. Yazdani, *Trans. Nonferrous Met. Soc. China*, **23**, 2551 (2013); https://doi.org/10.1016/S1003-6326(13)62767-3
49. M.H. Setianto and A.A. Korda, *J. Phys. Conf. Ser.*, **1204**, 012039 (2019); https://doi.org/10.1088/1742-6596/1204/1/012039
50. R. Wang, L. Wang, C. He, M. Lu and L. Sun, *Surf. Coat. Technol.*, **360**, 369 (2019); https://doi.org/10.1016/j.surfcoat.2018.12.092
51. V.R. Capelossi, M. Poelman, I. Recloux, R.P.B. Hernandez, H.G. de Melo and M.G. Olivier, *Electrochim. Acta*, **124**, 69 (2014); https://doi.org/10.1016/j.electacta.2013.09.004
52. M.Z. Mubarok, Wahab, Sutarno and S. Wahyudi, *J. Miner. Mater. Charact. Eng.*, **3**, 154 (2015); https://doi.org/10.4236/jmmce.2015.33018
53. R. Elaish, M. Curioni, K. Gowers, A. Kasuga, H. Habazaki, T. Hashimoto and P. Skeldon, *Surf. Coat. Techmol.*, **342**, 233 (2018); https://doi.org/10.1016/j.surfcoat.2018.02.096
54. M. Ji, W. Li, H. Liu, L. Zhu, H. Chen and W. Li, *Surf. Interfaces*, **19**, 100479 (2020); https://doi.org/10.1016/j.surfin.2020.100479
55. J. Lu, G. Wei, Y. Yu, C. Guo and L. Jiang, *Surf. Interfaces*, **13**, 46 (2018); https://doi.org/10.1016/j.surfin.2018.08.003
56. S. Somasundaram, A.M. Pillai, A. Rajendra, A. P, P.M. Krishna and A.K. Sharma, *Sol. Energy Mater. Sol. Cells*, **174**, 163 (2018); https://doi.org/10.1016/j.solmat.2017.08.023